

Feasibility of light scalars in a class of two-Higgs-doublet models and their decay signatures

Gautam Bhattacharyya¹, Dipankar Das¹, Anirban Kundu²

¹*Saha Institute of Nuclear Physics, 1/AF Bidhan Nagar, Kolkata 700064, India*

²*Department of Physics, University of Calcutta,
92 Acharya Prafulla Chandra Road, Kolkata 700009, India*

Abstract

We demonstrate that light charged and extra neutral scalars in the (100-200) GeV mass range pass the potentially dangerous flavor constraints in a particular class of two-Higgs-doublet model which has appropriately suppressed flavor-changing neutral currents at tree level. We study their decay branching ratios into various fermionic final states and comment on the possibility of their detection in the collider experiments. We also remark on how their trademark decay signatures can be used to discriminate them from the light nonstandard scalars predicted in other two-Higgs-doublet models.

1 Introduction

Plenty of motivations exist for considering the recently discovered Higgs boson at the CERN Large Hadron Collider (LHC) to be a member of a richer scalar structure beyond what is predicted by the Standard Model (SM). An exciting possibility is the two-Higgs-doublet model (2HDM) [1], which receives special attention because the minimal supersymmetric standard model relies on it. Extremely tight experimental constraints on tree level flavor-changing neutral currents (FCNC) led to the Glashow-Weinberg-Paschos theorem in the multi-Higgs context [2, 3]. This implies that the absence of tree level FCNC will be ensured if all right-handed fermions of a given charge couple to a single Higgs doublet. In 2HDM, this can be achieved by the introduction of discrete or continuous symmetries that act on the scalars and fermions. Following the Z_2 discrete symmetry under which $\Phi_1 \rightarrow -\Phi_1$ and $\Phi_2 \rightarrow \Phi_2$, four types of 2HDM emerge, based on the fermion transformations under that symmetry. They are classified as (i) Type I: all quarks and leptons couple to only one scalar Φ_2 ; (ii) Type II: Φ_2 couples to up-type quarks, while Φ_1 couples to down-type quarks and charged leptons (minimal supersymmetry conforms to this category); (iii) Type Y (or III, or flipped): Φ_2 couples to up-type quarks and leptons, while Φ_1 couples to down-type quarks; (iv) Type X (or IV, or lepton specific): Φ_2 couples to all quarks, while Φ_1 couples to all leptons. Experimental constraint on the charged Higgs mass in the Type II and Y models is quite strong: $m_{\xi^\pm} > 300$ GeV for any $\tan \beta \equiv v_2/v_1$, which is the ratio of the two vacuum expectation values. This arises mainly from the $b \rightarrow s\gamma$ constraint, but this constraint is considerably weak in Type I and X scenarios [4].

In this paper, we consider a special category of 2HDM formulated by Branco, Grimus and Lavoura (hereafter called the BGL scenario) [5], where tree level FCNC exists with appropriate suppression arising from the elements of the Cabibbo-Kobayashi-Maskawa (CKM) matrix¹. Unlike the general 2HDM with tree level FCNC [7, 8], the BGL models introduce no new parameters in the Yukawa sector, and therefore, are more predictive. In this scenario, instead of the discrete Z_2 symmetry a global U(1) symmetry acts on a particular generation i at a time, as follows:

$$Q_{Li} \rightarrow e^{i\theta} Q_{Li}, \quad u'_{Ri} \rightarrow e^{2i\theta} u'_{Ri}, \quad \Phi_2 \rightarrow e^{i\theta} \Phi_2. \quad (1)$$

Here $Q_{Li} = (u'_{Li}, d'_{Li})^T$ is the left-handed quark doublet for the i -th generation ($i = 1, 2, 3$), while u'_R denotes the up-type right-handed quark singlets, all in the weak basis. The scalar doublet Φ_1 and the other quark fields

¹A nonrenormalizable version of a similar scenario was constructed in [6].

remain unaffected by this transformation. For this particular choice of the symmetry, there will be no FCNC in the up sector and the FCNC in the down sector will be controlled by the i -th row of the CKM matrix. This will lead to three variants which will be called u-, c- and t-type models according to $i = 1, 2$, and 3 respectively². A number of low-energy observables severely constrain the u- and c-type models, as we will show later; so it makes sense to talk about the t-type model only. We will also show from the same observables that in the t-type model one can entertain charged Higgs mass in the ballpark of 150 GeV for $\tan \beta > 1$. In fact, the additional scalars, namely, the CP-even H and the CP-odd A together with the charged scalar ξ^+ , could all be taken in the 100-200 GeV mass range. These light scalars would leave distinct decay signatures in the collider experiments. By comparing their branching ratios in various flavor channels, it is possible to distinguish the BGL scalars from the light ones predicted in Type I and X models. Our study assumes special significance in view of the 14 TeV run of the LHC, its possible upgrade to higher luminosity, and the possibility of precision studies at the International Linear Collider (ILC).

The paper is arranged as follows. In Section II, we briefly introduce the BGL model. Section III deals with the low-energy constraints on the model. In particular, we show that the BGL model allows a light charged Higgs. We also point out the differences between BGL and other 2HDMs. The decay patterns and possible signatures of the nonstandard scalars are discussed in Section IV. We summarize and conclude in the last section. The appendices contain all the relevant formulae that have gone into our calculations.

2 Yukawa sector of 2HDM (BGL)

The scalar potential of the BGL model is identical to the other canonical 2HDMs. This scenario is manifestly CP conserving. Let us denote the CP-even neutral components of Φ_1 and Φ_2 by $\rho_1/\sqrt{2}$ and $\rho_2/\sqrt{2}$ respectively, with $\langle \rho_{1(2)} \rangle = v_{1(2)}$. They are of course weak eigenstates. The corresponding mass eigenstates H and h can be obtained by diagonalizing the 2×2 mass matrix \mathcal{M} using an orthogonal transformation characterized by an angle α , given by

$$\cos 2\alpha \equiv \frac{\mathcal{M}_{11} - \mathcal{M}_{22}}{\sqrt{(\mathcal{M}_{11} - \mathcal{M}_{22})^2 + 4\mathcal{M}_{12}^2}}. \quad (2)$$

By convention, we will take $m_h < m_H$, and h to be the 125 GeV scalar resonance discovered at the LHC.

To study the Yukawa sector of the BGL model, it is helpful to go to another neutral scalar basis $\{H^0, R\}$. This is not the mass basis in general, and is obtained from the $\{\rho_1, \rho_2\}$ basis by a rotation through the angle $\beta \equiv \tan^{-1}(v_2/v_1)$. The same rotation picks out the physical charged Higgs (ξ^+) and charged Goldstone (G^+), as well as the physical pseudoscalar (A) and neutral Goldstone (G^0), from their respective weak basis states. In the CP-even neutral sector, $\langle H^0 \rangle = v = \sqrt{v_1^2 + v_2^2} = 246$ GeV, while $\langle R \rangle = 0$. The relationship between the two bases $\{H, h\}$ and $\{H^0, R\}$ is given by

$$H^0 = \cos(\beta - \alpha)H + \sin(\beta - \alpha)h, \quad (3a)$$

$$R = -\sin(\beta - \alpha)H + \cos(\beta - \alpha)h. \quad (3b)$$

The H^0 state has gauge and Yukawa couplings identical to those of the SM Higgs boson. The physical state h , observed at the LHC, conforms to the state H^0 in the decoupling limit $\beta = \alpha \pm \pi/2$ [9]. This decoupling limit in the 2HDM context is now being increasingly motivated by the LHC data [10, 11].

The Yukawa Lagrangian of the BGL model, worked out in [5], is given by

$$\begin{aligned} \mathcal{L}_Y = & -\frac{1}{v}H^0 [\bar{d}D_d + \bar{u}D_u] + \frac{1}{v}R [\bar{d}(N_d P_R + N_d^\dagger P_L)d + \bar{u}(N_u P_R + N_u^\dagger P_L)u] \\ & + \frac{i}{v}A [\bar{d}(N_d P_R - N_d^\dagger P_L)d - \bar{u}(N_u P_R - N_u^\dagger P_L)u] + \left\{ \frac{\sqrt{2}}{v}\xi^+ \bar{u} (V N_d P_R - N_u^\dagger V P_L) d + \text{h.c.} \right\}. \quad (4) \end{aligned}$$

²The other three variants can be obtained by replacing u'_R in Eq. (1) with d'_R (down-type singlet), as a result of which there will be no FCNC in the down sector and the FCNC in the up sector will be controlled by the columns of the CKM matrix. We do not consider this scenario primarily because the FCNC in the up sector is less restrictive.

Here, u and d stand for 3-generation up and down quarks in mass basis, D_u and D_d are diagonal up and down mass matrices, and V is the CKM matrix. The matrices N_u and N_d , for the u-, c- and t-type models, have the following form (the (i, j) indices in N_d refer to (d, s, b) quarks and the superscripts in bold font refer to the model type):

$$N_u^{\mathbf{u}} = \text{diag}\{-m_u \cot \beta, m_c \tan \beta, m_t \tan \beta\}, \quad (N_d)_{ij}^{\mathbf{u}} = \tan \beta m_i \delta_{ij} - (\tan \beta + \cot \beta) V_{ui}^* V_{uj} m_j, \quad (5a)$$

$$N_u^{\mathbf{c}} = \text{diag}\{m_u \tan \beta, -m_c \cot \beta, m_t \tan \beta\}, \quad (N_d)_{ij}^{\mathbf{c}} = \tan \beta m_i \delta_{ij} - (\tan \beta + \cot \beta) V_{ci}^* V_{cj} m_j, \quad (5b)$$

$$N_u^{\mathbf{t}} = \text{diag}\{m_u \tan \beta, m_c \tan \beta, -m_t \cot \beta\}, \quad (N_d)_{ij}^{\mathbf{t}} = \tan \beta m_i \delta_{ij} - (\tan \beta + \cot \beta) V_{ti}^* V_{tj} m_j. \quad (5c)$$

In the leptonic sector (with only left-handed neutrinos), the Yukawa couplings of Eq. (4) should be read with the replacement $(N_u, D_u) \rightarrow 0$, $V = 1$, and $N_d(D_d) \rightarrow N_e(D_e)$, with N_e resembling the diagonal N_u matrices in Eq. (5) with appropriate replacement of quark masses by the charged lepton masses. This means that there is no FCNC in the leptonic sector when the neutrinos are considered to be massless.

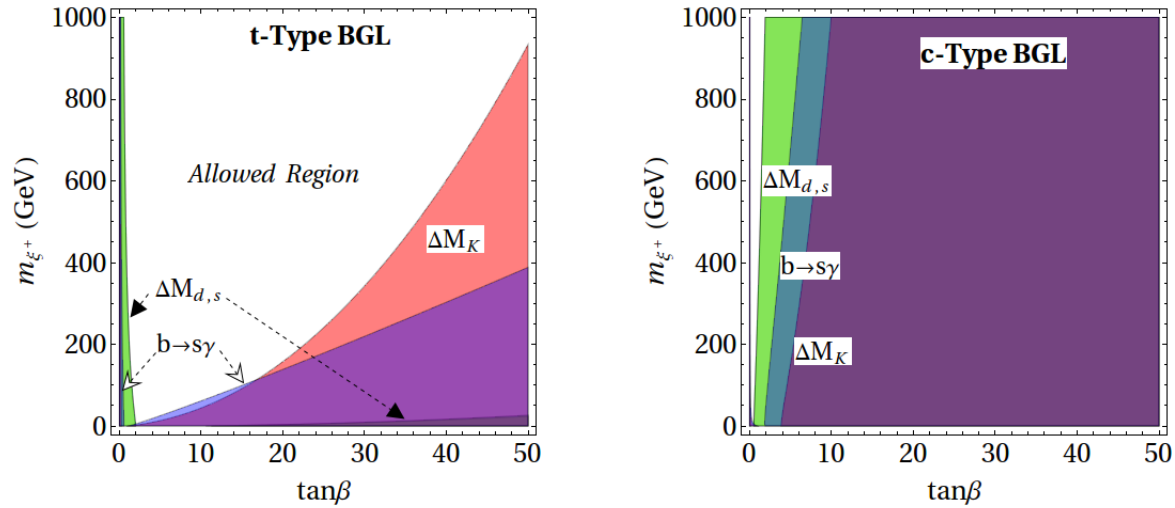


Figure 1: Constraints from various observables for t - and c -(u -) type BGL models. In the left panel (t -type), for large $\tan \beta$, ΔM_K offers a stronger constraint than $b \rightarrow s\gamma$. The vertical spiked shaded region in the extreme left also correspond to the entire disallowed region in Type I and X models. In the right panel (c - or u -types), ΔM_d and ΔM_s provide the most stringent constraints. Note that an assumption $m_H = m_A$ has been made to switch off the tree level contribution to the neutral meson mass differences.

The CP-odd scalar mass eigenstate A would be massless if the symmetry of Eq. (1) is exact in the Higgs potential. Thus, in the 't Hooft sense, a light pseudoscalar will be natural in these models. While there are five free parameters in any BGL model, namely, α , β , m_{ξ^+} , m_H , and m_A , we can make some reasonable simplifications. Considerations of perturbativity and stability of scalar potential ensure that $m_A \sim m_H$ if $\tan \beta \geq 10$ [12]. If m_A and m_H are large, we can even bring down the $\tan \beta$ limit further, say up to $\tan \beta = 5$. However, for the sake of simplicity and economy of parameters, we will assume $m_H = m_A$ for the remainder of this paper unless explicitly mentioned otherwise. Thus, in the decoupling limit, i.e. $\cos(\beta - \alpha) = 0$, we are left with only three unknown parameters: $\tan \beta$, m_{ξ^+} and $m_{H/A}$. It should be noted though that consistency with the oblique T -parameter requires $m_{\xi^+} \sim m_H$ once we assume $m_H = m_A$ [12].

3 Constraints on the parameter space

3.1 Neutral meson mixing

Neutral meson mass differences offer important constraints. The tree-level scalar exchange contribution to the off-diagonal element of the 2×2 Hamiltonian matrix is given by [5]

$$(M_{12}^K)^{\text{BGL}} \approx \frac{5}{24} \frac{f_K^2 m_K^3}{v^2} (V_{id}^* V_{is})^2 \frac{1}{\mathcal{A}^2}, \quad (6)$$

where m_K is the neutral kaon mass and f_K is the decay constant. Similar expressions exist for B_d and B_s systems. The mass difference is given by $\Delta M_K \approx 2|M_{12}^K|$. The contributions of three neutral scalars are contained in

$$\frac{1}{\mathcal{A}^2} = (\tan \beta + \cot \beta)^2 \left(\frac{\cos^2(\beta - \alpha)}{m_h^2} + \frac{\sin^2(\beta - \alpha)}{m_H^2} - \frac{1}{m_A^2} \right) = (\tan \beta + \cot \beta)^2 \left(\frac{1}{m_H^2} - \frac{1}{m_A^2} \right). \quad (7)$$

The last equality in Eq. (7) holds in the decoupling limit. The size of the prefactors in Eq. (6) tells us that $m_A = m_H$ is very well motivated from the neutral kaon mass difference for the u- and c-type models. For the t-type model, however, this degeneracy is more of an assumption than a requirement especially for $\tan \beta \sim 1$.

With the assumption $m_H = m_A$, the dominant contributions to neutral meson mass differences come from the charged Higgs box diagrams. The expressions for the loop-induced amplitudes are given explicitly in Appendix A. In Fig. 1, constraints have been placed assuming that the new physics contributions saturate the experimental values of ΔM [13]. For $\tan \beta > 1$, ΔM_d and ΔM_s severely restrict the u- and c-type models, whereas the t-type model can admit a light charged Higgs, at least for $m_H = m_A$. For large $\tan \beta$, ΔM_K offers a stronger constraint than $b \rightarrow s\gamma$ (discussed later) in the t-type model due to the dominance of the charm-induced box graph.

3.2 $b \rightarrow s\gamma$

The process $b \rightarrow s\gamma$ offers severe constraint on the charged Higgs mass [14, 15]. For Type II and Y models, in the charged Higgs Yukawa interaction, the up-type Yukawa coupling is multiplied by $\cot \beta$ while the down-type Yukawa is multiplied by $\tan \beta$. Their product is responsible for setting $\tan \beta$ -independent limit $m_{\xi^+} > 300$ GeV for $\tan \beta > 1$ [4, 16, 17]. In Type I and X models, each of these couplings picks up a $\cot \beta$ factor, which is why there is essentially no bound on charged Higgs mass for $\tan \beta > 1$ in these models [4].

In the BGL class of models, the constraint on m_{ξ^+} is different from that in Type I or Type X 2HDM (detailed expressions are displayed in Appendix B). This is because the BGL symmetry of Eq. (1) does not respect family universality. For the i -type BGL model, the relevant Yukawa couplings contain an overall factor of $(-\cot \beta)$ for vertices involving the i -th generation up-type fermion and a factor of $\tan \beta$ for the others. Consequently, the top loop contribution to the $b \rightarrow s\gamma$ amplitude will grow as $\tan^2 \beta$ for u- and c-type models resulting in very tight constraints on m_{ξ^+} for $\tan \beta > 1$. On the contrary, for t-type models, the top-loop contribution will decrease with increasing $\tan \beta$ and will hardly leave any effect for $\tan \beta > 1$, similar to what happens in the Type I and X models. But unlike in the latter scenarios, the charm loop amplitude in t-type BGL grows as $\tan^2 \beta$. It becomes numerically important for large $\tan \beta$ and does not allow ξ^+ to be very light.

Taking the branching ratio $\text{Br}(b \rightarrow s\gamma)_{\text{SM}} = (3.15 \pm 0.23) \times 10^{-4}$ [18–20] and $\text{Br}(b \rightarrow s\gamma)_{\text{exp}} = (3.55 \pm 0.26) \times 10^{-4}$ [21], these features of the BGL models have been displayed in Fig. 1. The regions excluded at 95% CL from $b \rightarrow s\gamma$ have been shaded and appropriately marked. Note that we have considered not only the contributions from (ξ^+, u_i) loops, but also from $(H/A, d_i)$ loops (due to tree level FCNC couplings of H and A). The numerical effects of the latter are found to be small; we refer the reader to Fig. 2, where separate contributions from the charged and the neutral scalars to C_{7L} and C_{8L} are shown. The behaviour can also be intuitively understood from the following comparison of the dominant contributions from the charged and neutral scalar induced loops to the $b \rightarrow s\gamma$ amplitude. The ratio of ξ^+ and (H/A) -induced loop

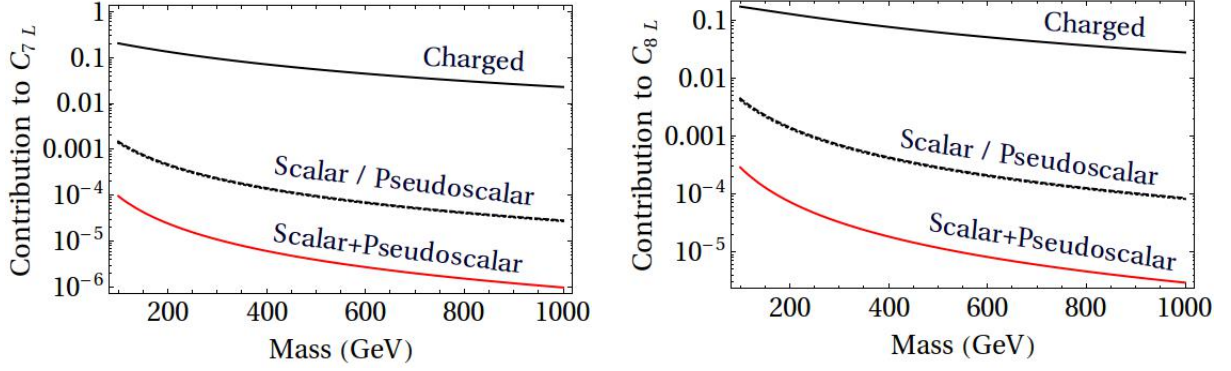


Figure 2: Magnitude of the contributions to the effective Wilson coefficients C_{7L} and C_{8L} for $b \rightarrow s\gamma$, coming from ξ^+ , H , and A , plotted against the corresponding masses. The middle curve in each panel shows the magnitude of the individual scalar and pseudoscalar contributions; they are too close to be differentiated in the shown scale. The lowest curve in each panel shows the sum of H and A contributions for the case $m_H = m_A$, which shows that the scalar and pseudoscalar contributions interfere destructively. C_{7R} and C_{8R} are suppressed by m_s/m_b and are not shown here.

contributions roughly goes like $(m_c^2 \tan^2 \beta / m_b m_s)$ for large $\tan \beta$, and $(m_t^2 \cot^2 \beta / m_b m_s)$ for $\tan \beta$ of the order of one. This justifies that the constraint from $b \rightarrow s\gamma$ essentially applies on the charged Higgs mass. In other words, that ξ^+ can be really light does not crucially depend on the values of m_H and m_A . From now on, we stick only to the t-type model to promote light charged Higgs phenomenology.

3.3 Other constraints

For t-type model, the branching ratios $\text{Br}(B \rightarrow D^{(*)}\tau\nu)$ and $\text{Br}(B^+ \rightarrow \tau\nu)$ do not receive any appreciable contributions unless the charged Higgs mass is unnaturally small defying the LEP2 direct search limit of 80 GeV [22]. The process $B_s \rightarrow \ell^+\ell^-$ proceeds at the tree level mediated by H/A providing important constraints. The amplitudes are proportional to $(\tan^2 \beta + 1)/m_{H/A}^2$ for $\ell = e, \mu$, and $(\cot^2 \beta + 1)/m_{H/A}^2$ for $\ell = \tau$. In Fig. 3 we have shaded the region excluded at 95% CL, obtained by comparing the SM expectation of $\text{Br}(B_s \rightarrow \mu^+\mu^-) = (3.65 \pm 0.23) \times 10^{-9}$ [23] with its experimental value $(3.2 \pm 1.0) \times 10^{-9}$ [24]. The details are provided in Appendix C. In the same plot we display different contours for $\text{Br}(B_s \rightarrow \tau^+\tau^-)/\text{Br}(B_s \rightarrow \tau^+\tau^-)_{\text{SM}}$, where we observe slight enhancement over the SM expectation.

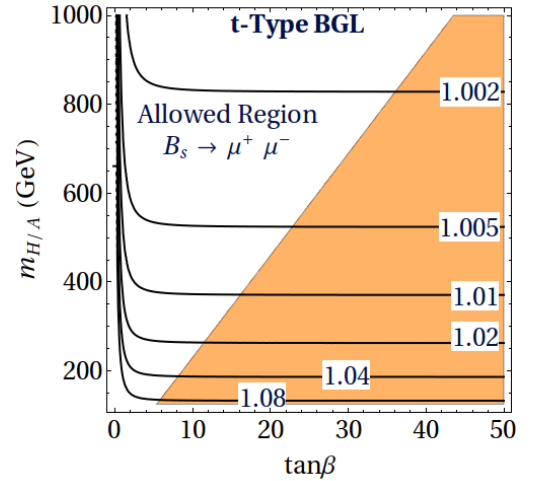


Figure 3: The shaded region is disallowed by $B_s \rightarrow \mu^+\mu^-$ at 95% CL. Contours of enhancements in $B_s \rightarrow \tau^+\tau^-$ over the SM estimate are also shown.

4 Charged and neutral scalar branching ratios

In Type I model, the light charged Higgs goes to $\tau\nu$ and cs (below the $t\bar{b}$ threshold), and the branching ratios are independent of $\tan \beta$, because both the leptonic and the quark couplings have the same $\cot \beta$ prefactor [25, 26].

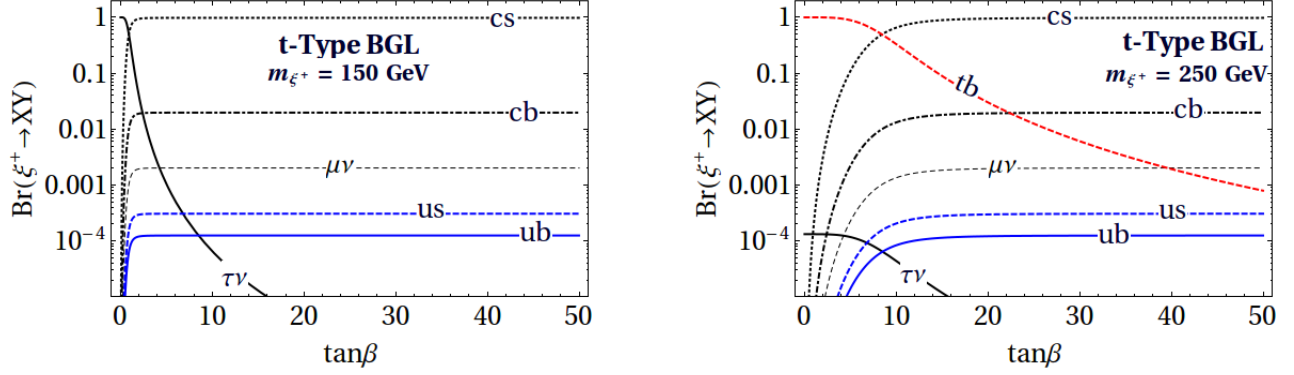


Figure 4: The charged Higgs branching ratios to two-body final states for two benchmark choices of m_{ξ^+} .

In Type X model, the leptonic part has an overall $\tan\beta$ multiplicative factor, so the charged Higgs preferentially decays into third generation leptonic channels for large $\tan\beta$ (e.g. almost entirely so for $\tan\beta \geq 2.5$). In the t-type BGL scenario, the charged Higgs branching ratios into two-body fermionic final states have been plotted in Fig. 4. We have considered two benchmark values for m_{ξ^+} , one below the tb threshold and the other well above it. To a good approximation it is enough to consider fermionic final states, because in the decoupling limit the $W^\pm h \xi^\mp$ coupling vanishes and if we consider near degeneracy of m_{ξ^+} and $m_{H/A}$ to satisfy the T -parameter constraint, then ξ^+ cannot decay into $W^+ S^0$ ($S^0 = H, A$) channel. Two noteworthy features which distinguish the t-type BGL model from others are: (i) the $\mu\nu$ final state dominates over $\tau\nu$ for $\tan\beta > 5$, which is a distinctive characteristic of t-type BGL model unlike any of the Type I, II, X or Y models (due to family nonuniversal BGL Yukawa couplings); (ii) for $\tan\beta > 10$, the branching ratio into cs significantly dominates over other channels including tb , again a unique feature of t-type BGL. The reason for the latter can be traced to the relative size of the top and charm quark masses *vis-à-vis* the $\tan\beta$ or $\cot\beta$ prefactor. This will result in a dijet final state at the LHC, without any b -jet, and hence the signal will be extremely difficult to be deciphered over the standard QCD background.

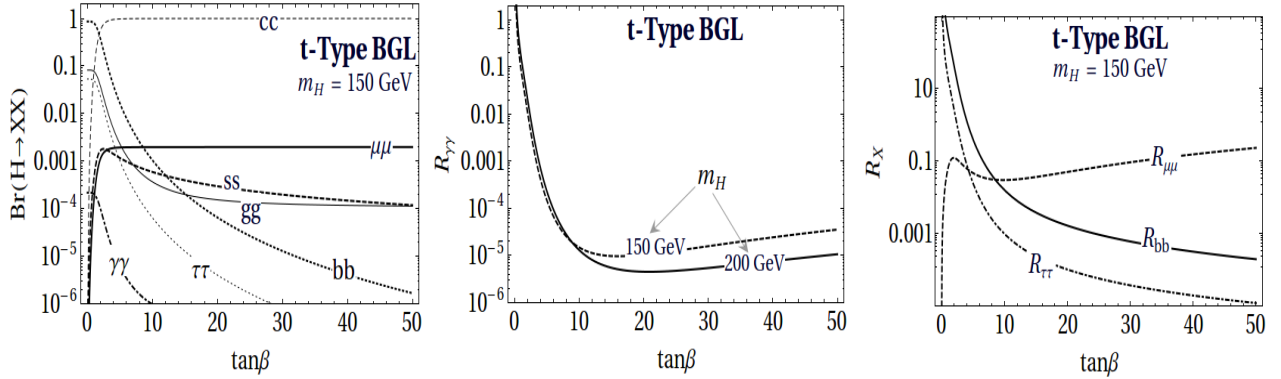


Figure 5: For various two-body final states, the R values, and the branching ratios of H .

We now discuss the decay branching ratios of the neutral scalar H . In the decoupling limit HVV ($V = W, Z$) coupling vanishes. Hence we discuss flavor diagonal ff final states (flavor violating modes are CKM suppressed), together with $\gamma\gamma$ and gg final states. In other types of 2HDM, the bb and $\tau\tau$ final states dominate over cc and $\mu\mu$ channels, respectively [26]. Here, the hierarchy is reversed, which transpires from the expressions of N_d and N_u in Eq. (5). To provide an intuitive estimate of the signal strength, we define the following variable:

$$R_X = \frac{\sigma(pp \rightarrow H \rightarrow X)}{\sigma(pp \rightarrow h \rightarrow \gamma\gamma)}, \quad (8)$$

where the normalization has been done with respect to the SM Higgs production and its diphoton decay branching ratio. We recall that the loop contributions of charged scalars to $h \rightarrow \gamma\gamma$ is tiny as long as $m_{H/A} \simeq m_{\xi^\pm}$ [12]. The relative merits of various channels have been plotted in Fig. 5. The crucial thing to observe is that although for $\tan\beta > 5$, H decays entirely into dijet (cc), the $\mu^+\mu^-$ mode may serve as a viable detection channel for H in future. With 20 fb^{-1} luminosity at LHC8, the expected number of diphoton events from the SM Higgs decay is about 400. Fig. 5 shows that $R_{\mu\mu} \sim 0.1$, i.e. about 40 dimuon events from H decay should have been observed. However, they are going to be swamped by huge background (mainly Drell-Yan, also QCD jets faking dimuon) [27]. At LHC14 with an integrated luminosity of 300 fb^{-1} , we expect about 39000 $h \rightarrow \gamma\gamma$ events [28], which means about 3900 $H \rightarrow \mu\mu$ events for $m_H = 150 \text{ GeV}$. Dimuon background studies at 14 TeV are not yet publicly available. A rough conservative extrapolation of the existing 7 and 8 TeV studies of the dimuon background [27] gives us hope that the signal can be deciphered over the background. Note that these are all crude estimates, made mainly to get our experimental colleagues interested in probing such exotic decay modes. A more careful study including, e.g. detection efficiencies and detailed background estimates, is beyond the scope of this paper. We emphasize that our scenario does not say that H, A or ξ^\pm have to be necessarily light. If they are heavy as they are forced to be in many other 2HDMs ($\sim 500 \text{ GeV}$ or more), their direct detection in early LHC14 would be that much difficult. The feature that makes our scenario unique is the *possibility* of their relative lightness as well as unconventional decay signatures.

5 Conclusions

We have shown that a particular class of two-Higgs-doublet model admits charged and additional neutral scalars which can be as light as $\sim 150 \text{ GeV}$. They successfully negotiate the stringent constraints from radiative b -decay, neutral meson mass differences, and dimuon decays of B mesons. Special features of Yukawa couplings in this model lead to characteristic decay signatures of the nonstandard scalars, which are different from the signatures of similar scalars in other 2HDM variants. Preferential decays of both the charged and additional neutral scalars into *second*, rather than the *third*, generation fermions for $\tan\beta > 5$ constitute the trademark distinguishing feature of this scenario, which can be tested in the high luminosity option of the LHC or at the ILC.

Note added: During the finalization of this manuscript, the paper [29] appeared which also deals with the BGL scenario. We agree with their overall conclusion on the feasibility of light charged Higgs boson. We have, however, additionally analyzed the decay signatures of the new scalars.

6 Acknowledgements

We thank Sunanda Banerjee and Swagata Mukherjee for helpful discussions. AK acknowledges Department of Science and Technology, Govt. of India, and Council for Scientific and Industrial Research, Govt. of India, for research support. DD thanks the Department of Atomic Energy, India, for financial support.

A Neutral meson mixing

The dominant one-loop effective Lagrangian for $\Delta F = 2$ is

$$\mathcal{L}_{\text{eff}}^{\Delta F=2} = \frac{G_F^2 M_W^2}{16\pi^2} \sum_{a,b=u,c,t} \lambda_a \lambda_b w_a w_b [S(w_a, w_b) + X_a X_b \{2I_1(w_a, w_b, w_\xi) + X_a X_b I_2(w_a, w_b, w_\xi)\}] O_F. \quad (\text{A.1})$$

Here, the $S(w_a, w_b)$ part is the SM contribution and the rest is due to the charged Higgs box diagrams. For i -type BGL model, $X_q = -\cot\beta$ if $q = i$ and $X_q = \tan\beta$ otherwise. The dimension-6 operator for $K^0-\bar{K}^0$

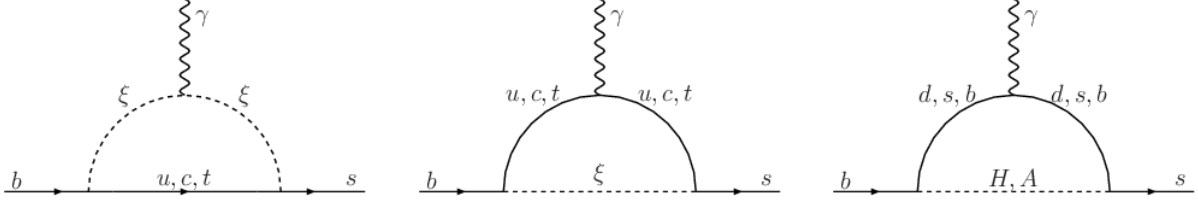


Figure 6: Feynman diagrams involving nonstandard scalars contributing to $b \rightarrow s\gamma$ amplitude.

mixing is

$$O_F = (\bar{s}\gamma^\mu P_L d)^2. \quad (\text{A.2})$$

Similar expressions can be obtained for B systems. The relevant parameters and functions are defined as follows:

$$\begin{aligned} \lambda_a &= V_{ad}^* V_{as}, \quad w_a = \frac{m_a^2}{M_W^2}, \quad f(x) = \frac{(x^2 - 8x + 4) \ln x + 3(x - 1)}{(x - 1)^2}, \\ S(w_a, w_b) &= \frac{f(w_a) - f(w_b)}{w_a - w_b}, \quad g(x, y, z) = \frac{x(x - 4) \ln x}{(x - 1)(x - y)(x - z)}, \\ I_1(w_a, w_b, w_\xi) &= [g(w_a, w_b, w_\xi) + g(w_b, w_\xi, w_a) + g(w_\xi, w_a, w_b)], \\ I_2(w_a, w_b, w_\xi) &= \frac{1}{w_a - w_b} \left[\frac{w_a^2 \ln w_a}{(w_\xi - w_a)^2} - \frac{w_b^2 \ln w_b}{(w_\xi - w_b)^2} \right] \\ &\quad + \frac{w_\xi [(w_\xi - w_a)(w_\xi - w_b) + \{2w_a w_b - w_\xi(w_a + w_b)\} \ln w_\xi]}{(w_\xi - w_a)^2 (w_\xi - w_b)^2}. \end{aligned} \quad (\text{A.3})$$

Obtaining M_{12} from the effective Lagrangian is straightforward. As an example, for K -meson system (with B_K as bag parameter),

$$M_{12}^K = -\frac{1}{2m_K} \langle K^0 | \mathcal{L}_{\text{eff}}^{\Delta F=2} | \bar{K}^0 \rangle, \quad (\text{A.4})$$

$$\text{with} \quad \langle K^0 | O_F | \bar{K}^0 \rangle = \frac{2}{3} f_K^2 m_K^2 B_K. \quad (\text{A.5})$$

B Expressions for $b \rightarrow s\gamma$

The effective Lagrangian for $b \rightarrow s\gamma$ can be written as

$$\begin{aligned} \mathcal{L}_{\text{eff}} &= \sqrt{\frac{G_F^2}{8\pi^3}} V_{ts}^* V_{tb} m_b [\sqrt{\alpha} \{C_{7L} \bar{s}_L \sigma^{\mu\nu} b_R + C_{7R} \bar{s}_R \sigma^{\mu\nu} b_L\} F_{\mu\nu} \\ &\quad \sqrt{\alpha_s} \{C_{8L} \bar{s}_L T_a \sigma^{\mu\nu} b_R + C_{8R} \bar{s}_R T_a \sigma^{\mu\nu} b_L\} G_{\mu\nu}^a] + \text{h.c.}, \end{aligned} \quad (\text{B.1})$$

where $F_{\mu\nu}$ and $G_{\mu\nu}^a$ are field strength tensors for photon and gluon, respectively, and T^a s are the SU(3) generators. The branching ratio $\text{Br}(b \rightarrow s\gamma)$ is given by

$$\frac{\text{Br}(b \rightarrow s\gamma)}{\text{Br}(b \rightarrow ce\bar{\nu})} = \frac{6\alpha}{\pi B} \left| \frac{V_{ts}^* V_{tb}}{V_{cb}} \right|^2 [|C_{7L}^{\text{eff}}|^2 + |C_{7R}^{\text{eff}}|^2], \quad (\text{B.2})$$

where, we have taken $B = 0.546$ [16]. The effective Wilson coefficients are

$$C_{7L}^{\text{eff}} = \eta^{16/23} C_{7L} + \frac{8}{3} (\eta^{14/23} - \eta^{16/23}) C_{8L} + \mathcal{C}, \quad (\text{B.3a})$$

$$C_{7R}^{\text{eff}} = \eta^{16/23} C_{7R} + \frac{8}{3} (\eta^{14/23} - \eta^{16/23}) C_{8R}. \quad (\text{B.3b})$$

In the above equations, $\eta = \alpha_s(M_Z)/\alpha_s(\mu)$, where μ is the QCD renormalization scale; \mathcal{C} corresponds to the leading log QCD corrections in SM. In the expression for the effective Wilson co-efficients (Eq. (B.3)), the correction term is given by

$$\mathcal{C} = \sum_{i=1}^8 h_i \eta^{a_i}, \quad (\text{B.4})$$

where,

$$\begin{aligned} a_i &= \left(\frac{14}{23}, \frac{16}{23}, \frac{6}{23}, -\frac{12}{23}, 0.4086, -0.4230, -0.8994, 0.1456 \right), \\ h_i &= \left(\frac{626126}{272277}, -\frac{56281}{51730}, -\frac{3}{7}, -\frac{1}{14}, -0.6494, -0.0380, -0.0186, -0.0057 \right). \end{aligned} \quad (\text{B.5})$$

The values of h_i and a_i can be found in [18] [see Eq. (2.3) and Table 1 of Ref. [18]].

To understand the above expressions, we first define the following functions:

$$\begin{aligned} \mathcal{F}_0(t) &= \int_0^1 dx \frac{1-x}{x+(1-x)t} = -\frac{1}{1-t} - \frac{\ln t}{(1-t)^2}, \\ \mathcal{F}_1(t) &= \int_0^1 dx \frac{(1-x)^2}{x+(1-x)t} = \frac{-3+4t-t^2}{2(1-t)^3} - \frac{\ln t}{(1-t)^3}, \\ \mathcal{F}_2(t) &= \int_0^1 dx \frac{(1-x)^3}{x+(1-x)t} = \frac{-11+18t-9t^2+2t^3-6\ln t}{6(1-t)^4}, \\ \bar{\mathcal{F}}_0(t) &= \int_0^1 dx \frac{x}{x+(1-x)t} = \frac{1-t+t\ln t}{(1-t)^2}, \\ \bar{\mathcal{F}}_1(t) &= \int_0^1 dx \frac{x^2}{x+(1-x)t} = \frac{1-4t+3t^2-2t^2\ln t}{2(1-t)^3}, \\ \bar{\mathcal{F}}_2(t) &= \int_0^1 dx \frac{x^3}{x+(1-x)t} = \frac{2-9t+18t^2-11t^3+6t^3\ln t}{6(1-t)^4}. \end{aligned} \quad (\text{B.6})$$

Let us further define $x_t = m_t^2/m_W^2$, $y_q = m_q^2/m_\xi^2$, $z_q = m_q^2/m_H^2$, $z'_q = m_q^2/m_A^2$. Now the expressions for C_{7L} , C_{7R} , C_{8L} , C_{8R} read

$$\begin{aligned} C_{7L} &= A_\gamma^{\text{SM}} + A_\gamma^\xi + \frac{Q_b}{V_{ts}^* V_{tb}} \sum_{q=b,s} [A_L^H(z_q) + A_L^A(z'_q)], \\ C_{7R} &= \frac{m_s}{m_b} A_\gamma^{\text{SM}} + \frac{m_s}{m_b} A_\gamma^\xi + \frac{Q_b}{V_{ts}^* V_{tb}} \sum_{q=b,s} [A_R^H(z_q) + A_R^A(z'_q)], \\ C_{8L} &= A_g^{\text{SM}} + A_g^\xi + \frac{1}{V_{ts}^* V_{tb}} \sum_{q=b,s} [A_L^H(z_q) + A_L^A(z'_q)], \\ C_{8R} &= \frac{m_s}{m_b} A_g^{\text{SM}} + \frac{m_s}{m_b} A_g^\xi + \frac{1}{V_{ts}^* V_{tb}} \sum_{q=b,s} [A_R^H(z_q) + A_R^A(z'_q)]. \end{aligned} \quad (\text{B.7})$$

The SM and the new physics contributions (see Fig. 6) are given below :

■ SM :

$$\begin{aligned}
A_\gamma^{\text{SM}} &= \frac{1}{2} \left[\bar{\mathcal{F}}_1(x_t) + \bar{\mathcal{F}}_2(x_t) + \frac{1}{2} x_t \bar{\mathcal{F}}_2(x_t) - \frac{3}{2} x_t \bar{\mathcal{F}}_1(x_t) + x_t \bar{\mathcal{F}}_0(x_t) \right. \\
&\quad \left. + \frac{4}{3} \mathcal{F}_0(x_t) - 2 \mathcal{F}_1(x_t) + \frac{2}{3} \mathcal{F}_2(x_t) + \frac{1}{3} x_t \mathcal{F}_1(x_t) + \frac{1}{3} x_t \mathcal{F}_2(x_t) \right] - \frac{23}{36}, \\
A_g^{\text{SM}} &= \frac{1}{2} \left[2 \mathcal{F}_0(x_t) - 3 \mathcal{F}_1(x_t) + \mathcal{F}_2(x_t) + \frac{1}{2} x_t \mathcal{F}_1(x_t) + \frac{1}{2} x_t \mathcal{F}_2(x_t) \right] - \frac{1}{3},
\end{aligned} \tag{B.8}$$

■ Charged Higgs :

$$\begin{aligned}
A_g^\xi &= \frac{1}{4V_{ts}^* V_{tb}} \sum_{q=u,c,t} V_{qs}^* V_{qb} X_q^2 [y_q \mathcal{F}_1(y_q) + y_q \mathcal{F}_2(y_q)], \\
A_\gamma^\xi &= \frac{1}{V_{ts}^* V_{tb}} \sum_{q=u,c,t} V_{qs}^* V_{qb} X_q^2 C(y_q),
\end{aligned} \tag{B.9}$$

with

$$C(y) = \frac{1}{2} \left[\frac{1}{2} y \bar{\mathcal{F}}_2(y) - \frac{3}{2} y \bar{\mathcal{F}}_1(y) + y \bar{\mathcal{F}}_0(y) + \frac{1}{3} y \mathcal{F}_1(y) + \frac{1}{3} y \mathcal{F}_2(y) \right], \tag{B.10}$$

and for i -type model, $X_q = -\cot \beta$ if $q = i$ and $X_q = \tan \beta$ otherwise (e.g. for t -type model, $X_u = X_c = \tan \beta$, $X_t = -\cot \beta$).

■ CP-even Higgs :

$$\begin{aligned}
A_L^H(z_b) &= -\frac{1}{8} \left[\{z_b \mathcal{F}_1(z_b) - z_b \mathcal{F}_2(z_b)\} \left(\frac{AD}{m_b^2} + \frac{BC}{m_b^2} \frac{m_s}{m_b} \right) + 2z_b \mathcal{F}_1(z_b) \frac{AC}{m_b^2} \right], \\
A_R^H(z_b) &= -\frac{1}{8} \left[\{z_b \mathcal{F}_1(z_b) - z_b \mathcal{F}_2(z_b)\} \left(\frac{AD}{m_b^2} \frac{m_s}{m_b} + \frac{BC}{m_b^2} \right) + 2z_b \mathcal{F}_1(z_b) \frac{BD}{m_b^2} \right],
\end{aligned} \tag{B.11}$$

with $A = (N_d)_{sb}$, $B = (N_d)_{bs}^*$, $C = (N_d)_{bb}$, $D = (N_d)_{bb}^*$.

$$\begin{aligned}
A_L^H(z_s) &= -\frac{1}{8} \left[\{z_s \mathcal{F}_1(z_s) - z_s \mathcal{F}_2(z_s)\} \left(\frac{AD}{m_s^2} + \frac{BC}{m_s^2} \frac{m_s}{m_b} \right) + 2z_s \mathcal{F}_1(z_s) \frac{AC}{m_s^2} \frac{m_s}{m_b} \right], \\
A_R^H(z_s) &= -\frac{1}{8} \left[\{z_s \mathcal{F}_1(z_s) - z_s \mathcal{F}_2(z_s)\} \left(\frac{AD}{m_s^2} \frac{m_s}{m_b} + \frac{BC}{m_s^2} \right) + 2z_s \mathcal{F}_1(z_s) \frac{BD}{m_s^2} \frac{m_s}{m_b} \right],
\end{aligned} \tag{B.12}$$

with $A = (N_d)_{ss}$, $B = (N_d)_{ss}^*$, $C = (N_d)_{sb}$, $D = (N_d)_{bs}^*$.

■ CP-odd Higgs :

$$\begin{aligned}
A_L^A(z'_b) &= \frac{1}{8} \left[\{z'_b \mathcal{F}_1(z'_b) - z'_b \mathcal{F}_2(z'_b)\} \left(\frac{AD}{m_b^2} + \frac{BC}{m_b^2} \frac{m_s}{m_b} \right) + 2z'_b \mathcal{F}_1(z'_b) \frac{AC}{m_b^2} \right], \\
A_R^A(z'_b) &= \frac{1}{8} \left[\{z'_b \mathcal{F}_1(z'_b) - z'_b \mathcal{F}_2(z'_b)\} \left(\frac{AD}{m_b^2} \frac{m_s}{m_b} + \frac{BC}{m_b^2} \right) + 2z'_b \mathcal{F}_1(z'_b) \frac{BD}{m_b^2} \right],
\end{aligned} \tag{B.13}$$

with $A = (N_d)_{sb}$, $B = -(N_d)_{bs}^*$, $C = (N_d)_{bb}$, $D = -(N_d)_{bb}^*$.

$$\begin{aligned}
A_L^A(z'_s) &= \frac{1}{8} \left[\{z'_s \mathcal{F}_1(z'_s) - z'_s \mathcal{F}_2(z'_s)\} \left(\frac{AD}{m_s^2} + \frac{BC}{m_s^2} \frac{m_s}{m_b} \right) + 2z'_s \mathcal{F}_1(z'_s) \frac{AC}{m_s^2} \frac{m_s}{m_b} \right], \\
A_R^A(z'_s) &= \frac{1}{8} \left[\{z'_s \mathcal{F}_1(z'_s) - z'_s \mathcal{F}_2(z'_s)\} \left(\frac{AD}{m_s^2} \frac{m_s}{m_b} + \frac{BC}{m_s^2} \right) + 2z'_s \mathcal{F}_1(z'_s) \frac{BD}{m_s^2} \frac{m_s}{m_b} \right],
\end{aligned} \tag{B.14}$$

with $A = (N_d)_{ss}$, $B = -(N_d)_{ss}^*$, $C = (N_d)_{sb}$, $D = -(N_d)_{bs}^*$.

C $B_s \rightarrow \mu^+ \mu^-$

The effective Hamiltonian is

$$\mathcal{H}_{\text{eff}} = C_A^{bs} O_A^{bs} + C_S^{bs} O_S^{bs} + C_P^{bs} O_P^{bs}, \quad (\text{C.1})$$

with

$$O_A^{bs} = (\bar{b} \gamma_\alpha P_L s)(\bar{\mu} \gamma^\alpha \gamma_5 \mu), \quad O_S^{bs} = m_b (\bar{b} P_L s)(\bar{\mu} \mu), \quad O_P^{bs} = m_b (\bar{b} P_L s)(\bar{\mu} \gamma_5 \mu). \quad (\text{C.2})$$

Note that in addition to the above operators, there will be operators of the form $(\bar{b} P_R s)(\bar{\mu} \mu)$ and $(\bar{b} P_R s)(\bar{\mu} \gamma_5 \mu)$. But the Wilson coefficients corresponding to these operators will be proportional to m_s (instead of m_b) and their contribution can be neglected ($m_b \gg m_s$) as argued in [30]. With this assumption we can write

$$\frac{\text{Br}(B_s \rightarrow \mu^+ \mu^-)}{\text{Br}(B_s \rightarrow \mu^+ \mu^-)_{\text{SM}}} = \left\{ \left| 1 - m_{B_s}^2 \frac{C_P^{bs}}{2m_\mu C_A^{bs}} \right|^2 + m_{B_s}^4 \left(1 - \frac{4m_\mu^2}{m_{B_s}^2} \right) \left| \frac{C_S^{bs}}{2m_\mu C_A^{bs}} \right|^2 \right\} \times \frac{\Gamma_B^{\text{SM}}}{\Gamma_B}. \quad (\text{C.3})$$

The relevant part of the Lagrangian to evaluate C_S^{bs} and C_P^{bs} is

$$\begin{aligned} \mathcal{L}_{\text{quark}} &= \frac{R}{v} \bar{d}(N_d P_R + N_d^\dagger P_L) d + i \frac{A}{v} \bar{d}(N_d P_R - N_d^\dagger P_L) d \\ &= (N_d^\dagger)_{bs} \frac{R}{v} \bar{b} P_L s - i (N_d^\dagger)_{bs} \frac{A}{v} \bar{b} P_L s \\ &= (N_d^\dagger)_{bs} \frac{h}{v} \cos(\beta - \alpha) \bar{b} P_L s - (N_d^\dagger)_{bs} \frac{H}{v} \sin(\beta - \alpha) \bar{b} P_L s - i (N_d^\dagger)_{bs} \frac{A}{v} \bar{b} P_L s, \end{aligned} \quad (\text{C.4})$$

$$\begin{aligned} \mathcal{L}_{\text{lepton}} &= -\frac{H^0}{v} \bar{e} D_e e + \frac{R}{v} \bar{e}(N_e P_R + N_e^\dagger P_L) e + i \frac{A}{v} \bar{e}(N_e P_R - N_e^\dagger P_L) e \\ &= -\frac{m_\mu}{v} \bar{\mu} \mu H^0 + \frac{(N_e)_{\mu\mu}}{v} \bar{\mu} \mu R + \frac{i(N_e)_{\mu\mu}}{v} \bar{\mu} \gamma_5 \mu A \\ &= \left[\frac{h}{v} \{ -\sin(\beta - \alpha) m_\mu + \cos(\beta - \alpha) (N_e)_{\mu\mu} \} + \frac{H}{v} \{ -\cos(\beta - \alpha) m_\mu - \sin(\beta - \alpha) (N_e)_{\mu\mu} \} \right] \bar{\mu} \mu \\ &\quad + i \frac{A}{v} (N_e)_{\mu\mu} \bar{\mu} \gamma_5 \mu. \end{aligned} \quad (\text{C.5})$$

Note that terms involving $\bar{b} P_R s$ have not been displayed. Their coefficients are proportional to $(N_d)_{bs}$, which is proportional to m_s , and are therefore neglected.

$$(N_d)_{bs} = -(\tan \beta + \cot \beta) V_{ib}^* V_{is} m_s, \quad (\text{C.6a})$$

$$(N_d^\dagger)_{bs} = (N_d)_{sb}^* = -(\tan \beta + \cot \beta) V_{ib}^* V_{is} m_b. \quad (\text{C.6b})$$

The Wilson coefficients are

$$\begin{aligned} C_S^{bs} &= (\tan \beta + \cot \beta) \frac{V_{ib}^* V_{is}}{v^2} \left\{ \frac{\cos(\beta - \alpha)}{m_h^2} [-\sin(\beta - \alpha) m_\mu + \cos(\beta - \alpha) (N_e)_{\mu\mu}] \right. \\ &\quad \left. + \frac{\sin(\beta - \alpha)}{m_H^2} [\cos(\beta - \alpha) m_\mu + \sin(\beta - \alpha) (N_e)_{\mu\mu}] \right\}, \end{aligned} \quad (\text{C.7})$$

and

$$C_P^{bs} = (\tan \beta + \cot \beta) \frac{V_{ib}^* V_{is}}{v^2} \frac{(N_e)_{\mu\mu}}{m_A^2}. \quad (\text{C.8})$$

The SM Wilson coefficient is [30]

$$C_A^{bs} = \frac{\alpha G_F}{2\sqrt{2}\pi \sin^2 \theta_w} V_{tb}^* V_{ts} 2Y(x_t), \quad Y(x_t) = 0.997 \left[\frac{m_t(m_t)}{166 \text{ GeV}} \right]^{1.55} \approx 1.0. \quad (\text{C.9})$$

D Leptonic and semileptonic decays

The ratios $R(D)$ and $R(D^*)$ are defined as

$$R(D^{(*)}) = \frac{\text{Br}(B \rightarrow D^{(*)}\tau\nu)}{\text{Br}(B \rightarrow D^{(*)}\ell\nu)}, \quad (\text{D.1})$$

where $\ell = e, \mu$. The relevant expressions are [31]:

$$\begin{aligned} \frac{R(D)}{R(D)_{\text{SM}}} &= 1 + 1.5\text{Re}\left(\frac{C_R^{cb} + C_L^{cb}}{C_{\text{SM}}^{cb}}\right) + 1.0\left|\frac{C_R^{cb} + C_L^{cb}}{C_{\text{SM}}^{cb}}\right|^2, \\ \frac{R(D^*)}{R(D^*)_{\text{SM}}} &= 1 + 0.12\text{Re}\left(\frac{C_R^{cb} - C_L^{cb}}{C_{\text{SM}}^{cb}}\right) + 0.05\left|\frac{C_R^{cb} - C_L^{cb}}{C_{\text{SM}}^{cb}}\right|^2, \\ \frac{\text{Br}(B \rightarrow \tau\nu)}{\text{Br}(B \rightarrow \tau\nu)_{\text{SM}}} &= \left|1 + \frac{m_B^2}{m_b m_\tau} \frac{(C_R^{ub} - C_L^{ub})}{C_{\text{SM}}^{ub}}\right|^2, \end{aligned} \quad (\text{D.2})$$

where we have assumed no appreciable change in the B -meson lifetime due to this new interaction. The Wilson coefficients, as defined in the effective Hamiltonian in Ref. [31], are

$$\begin{aligned} C_{\text{SM}}^{qb} &= 2\sqrt{2}G_F V_{qb}, \\ -C_R^{qb} &= \frac{2}{v^2 m_\xi^2} (V N_d)_{qb} (N_e^\dagger)_{\tau\tau}, \\ -C_L^{qb} &= -\frac{2}{v^2 m_\xi^2} (N_u^\dagger V)_{qb} (N_e^\dagger)_{\tau\tau}, \end{aligned} \quad (\text{D.3})$$

where the extra minus sign in the last two lines comes from the nature of the propagator. For t-type model,

$$\begin{aligned} (N_e)_{\tau\tau} &= -m_\tau \cot \beta, \\ (N_u^\dagger V)_{ub} &= m_u \tan \beta V_{ub}; \quad (N_u^\dagger V)_{cb} = m_c \tan \beta V_{cb}, \\ (V N_d)_{ub} &= m_b \tan \beta V_{ub}; \quad (V N_d)_{cb} = m_b \tan \beta V_{cb}. \end{aligned} \quad (\text{D.4})$$

Thus, none of the above decay widths depend on $\tan \beta$ for t-type model.

References

- [1] G. C. Branco, P. M. Ferreira, L. Lavoura, M. N. Rebelo, M. Sher and J. P. Silva, Phys. Rept. **516**, 1 (2012) [arXiv:1106.0034 [hep-ph]].
- [2] S. L. Glashow and S. Weinberg, Phys. Rev. D **15**, 1958 (1977).
- [3] E. A. Paschos, Phys. Rev. D **15**, 1966 (1977).
- [4] F. Mahmoudi and O. Stal, Phys. Rev. D **81**, 035016 (2010) [arXiv:0907.1791 [hep-ph]].
- [5] G. C. Branco, W. Grimus and L. Lavoura, Phys. Lett. B **380**, 119 (1996) [hep-ph/9601383].
- [6] A. M. Hadeed and B. Holdom, Phys. Lett. B **159**, 379 (1985).
- [7] A. Crivellin, A. Kokulu and C. Greub, Phys. Rev. D **87**, 094031 (2013) [arXiv:1303.5877 [hep-ph]].
- [8] D. Atwood, L. Reina and A. Soni, Phys. Rev. D **55**, 3156 (1997) [hep-ph/9609279].
- [9] J. F. Gunion and H. E. Haber, Phys. Rev. D **67**, 075019 (2003) [hep-ph/0207010].

- [10] O. Eberhardt, U. Nierste and M. Wiebusch, JHEP **1307**, 118 (2013) [arXiv:1305.1649 [hep-ph]].
- [11] N. Craig, J. Galloway and S. Thomas, arXiv:1305.2424 [hep-ph].
- [12] G. Bhattacharyya, D. Das, P. B. Pal and M. N. Rebelo, JHEP **1310**, 081 (2013) [arXiv:1308.4297 [hep-ph]].
- [13] J. Beringer *et al.* [Particle Data Group Collaboration], Phys. Rev. D **86**, 010001 (2012).
- [14] B. Grinstein and M. B. Wise, Phys. Lett. B **201**, 274 (1988).
- [15] F. Borzumati and C. Greub, Phys. Rev. D **58**, 074004 (1998) [hep-ph/9802391].
- [16] O. Deschamps, S. Descotes-Genon, S. Monteil, V. Niess, S. T’Jampens and V. Tisserand, Phys. Rev. D **82**, 073012 (2010) [arXiv:0907.5135 [hep-ph]].
- [17] X. -D. Cheng, Y. -D. Yang and X. -B. Yuan, arXiv:1401.6657 [hep-ph].
- [18] P. Gambino and M. Misiak, Nucl. Phys. B **611**, 338 (2001) [hep-ph/0104034].
- [19] M. Misiak, H. M. Asatrian, K. Bieri, M. Czakon, A. Czarnecki, T. Ewerth, A. Ferroglia and P. Gambino *et al.*, Phys. Rev. Lett. **98**, 022002 (2007) [hep-ph/0609232].
- [20] M. Misiak and M. Steinhauser, Nucl. Phys. B **764**, 62 (2007) [hep-ph/0609241].
- [21] Y. Amhis *et al.* [Heavy Flavor Averaging Group Collaboration], arXiv:1207.1158 [hep-ex].
- [22] LEP Higgs Working Group for Higgs boson searches and ALEPH and DELPHI and L3 and OPAL Collaborations, hep-ex/0107031.
- [23] C. Bobeth, M. Gorbahn, T. Hermann, M. Misiak, E. Stamou and M. Steinhauser, arXiv:1311.0903 [hep-ph].
- [24] HFAG Website, <http://www.slac.stanford.edu/xorg/hfag/rare/2013/bs/OUTPUT/TABLES/bs.pdf>
- [25] M. Aoki, R. Guedes, S. Kanemura, S. Moretti, R. Santos and K. Yagyu, Phys. Rev. D **84**, 055028 (2011) [arXiv:1104.3178 [hep-ph]].
- [26] M. Aoki, S. Kanemura, K. Tsumura and K. Yagyu, Phys. Rev. D **80**, 015017 (2009) [arXiv:0902.4665 [hep-ph]].
- [27] The CMS Collaboration,
<http://cms-physics.web.cern.ch/cms-physics/public/HIG-13-007-pas.pdf>
The ATLAS Collaboration,
<https://cds.cern.ch/record/1523695/files/ATLAS-CONF-2013-010.pdf>
- [28] See the link: <https://twiki.cern.ch/twiki/bin/view/LHCPhysics/CERNYellowReportPageAt14TeV>
- [29] F. J. Botella, G. C. Branco, A. Carmona, M. Nebot, L. Pedro and M. N. Rebelo, arXiv:1401.6147 [hep-ph].
- [30] H. E. Logan and U. Nierste, Nucl. Phys. B **586**, 39 (2000) [hep-ph/0004139].
- [31] A. Crivellin, C. Greub and A. Kokulu, Phys. Rev. D **86**, 054014 (2012) [arXiv:1206.2634].